Experimental and Theoretical Studies on the Corrosion Inhibition Potentials of some Anisole derivatives for Mild Steel

N. O. Eddy[1], B. I. Ita[2], E. E. Ebenso[3,]*

[1] Department of Chemistry, Ahmadu Bello University, Zaria, Nigeria
[2] Department of Chemistry, University of Calabar, Calabar, Nigeria
[3] Department of Chemistry, School of Mathematical & Physical Sciences, North West University (Mafikeng Campus), Private Bag X2046, Mmabatho 2735, South Africa
[*]Corresponding author - E-mail: Eno.Ebenso@nwu.ac.za

The inhibitory and adsorption potentials of 2-(4-methoxybenzylideneamino) acetic acid (MBDAC), 2-hydroxy-3-methoxybenzaldehyde (HMBA) and 4-methoxybenzaldehyde (MBA) were studied using experimental (gravimetric and gasometric) and computational chemistry simulation approaches. The results obtained from the experimental approach revealed that the trend for the inhibitory potentials of the three anisoles is HMBA > MBDAC > MBA. The observed trend is attributed to the structural differences resulting from the introduction of $-OH$, $=O$ and NCH_2CO_2H substituents into the respective compounds. The adsorption of the three inhibitors on mild steel surface is spontaneous and supported the mechanism of chemical adsorption. Computational chemistry simulations was carried out by comparing calculated quantum chemical parameters (the energy of the frontier molecular orbitals, the energy gap, dipole moment and logP) of the studied anisoles in gas and aqueous phases with experimentally obtained % inhibition efficiencies. The tests gave excellent correlations for PM6, PM3, AM1, RM1 and MNDO Hamiltonians. Correlations between experimental and predicted inhibition efficiencies were also excellent. Local selectivity study using the Fukui function and global softness indices indicated that the likely sites for electrophilic and nucleophilic attacks are in the enol bonds of the inhibitors.

Keywords: Mild steel, corrosion inhibition, anisole derivatives, adsorption

1. INTRODUCTION

Mild steel is one of the most valuable metals in industries because of its high malleability and ductility. However, the metal is often prone to corrosion especially during industrial processes involving etching, acid washing and pickling of metals [1-2]. Due to the challenges posed by the corrosion of metals, several steps have been designed to protect metals against corrosion. However,

one of the best options involves the use of corrosion inhibitors [3]. A corrosion inhibitor retards the rate of corrosion of a metal by being adsorbed on its surface through the transfer of charge/electron from the inhibitor to the metal surface [4].
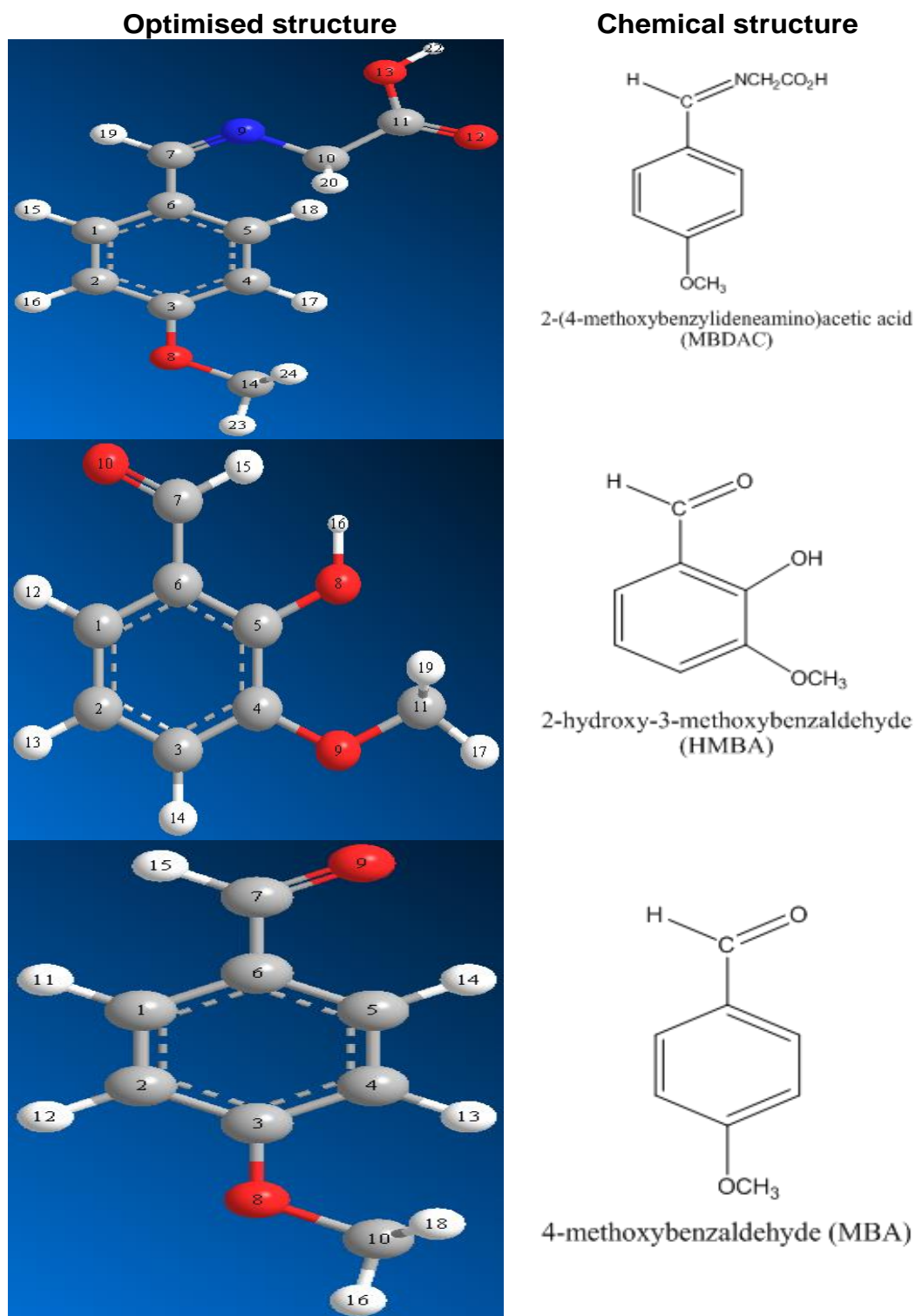
Figure 1. Chemical and optimised structures of MBDAC, HMBA and MBA

The choice of an inhibitor can be considered in two folds. Firstly, some inhibitors are obtained from living organisms and are referred to as green corrosion inhibitors [5]. Secondly, compounds containing hetero atoms in their aromatic or long carbon chain are capable of being adsorbed on the metal surface and can protect the metal against corrosion. For this class of compounds, the presence of hetero atoms as well as π-electrons in their double or triple bonds have been found to facilitate the adsorption of the metal [6,7].

In spite of the broad spectrum of inhibitors that have been tested and used for the inhibition of the corrosion of mild steel, literature is scanty on the use of anisole or its derivatives as inhibitors for mild steel corrosion. Therefore, the present study is aimed at investigating the corrosion inhibitory potentials of three anisole derivatives namely, 2-(4-methoxybenzylideneamino) acetic acid (MBDAC), 2-hydroxy-3-methoxybenzaldehyde (HMBA) and 4-methoxybenzaldehyde (MBA) (Fig. 1). The inhibitory potentials of these compounds shall be investigated using experimental techniques (gravimetric and gasometric techniques) and computational chemistry simulation. The results obtained from the two approaches shall be compared and the sites for electrophilic and nucleophilic attacks shall be established using Fukui function and global softness indices.

2. MATERIALS AND METHODS

2.1. Materials

Materials used for the study were mild steel coupon (dimension, 5x4x0.11cm and composition (wt %); Mn (0.6), P (0.36), C (0.15) and Si (0.03) and the rest Fe). Each coupon was degreased by washing with ethanol, dipped in acetone and allowed to dry in the air before they were preserved in a desicator. The concentrations range for the used inhibitors was 1×10^{-3} to 5×10^{-3} M.

2.2. Gravimetric method

In the gravimetric experiment, a previously weighed metal (mild steel) coupon was completely immersed in 250 ml of the test solution in an open beaker. The beaker was covered with aluminium foil and was inserted into a water bath maintained at 303 K. After every 24 hours, the corrosion product was removed by washing each coupon (withdrawn from the test solution) in a solution containing 50 % NaOH and 100 g l^{-1} of zinc dust. The washed coupon was rinsed in acetone and dried in the air before re-weighing. The experiment was also repeated at 333 K. In each case, the difference in weight for a period of 168 h was taken as the total weight loss. From the average weight loss results (average of three replicate analysis), the inhibition efficiency (IE_{exp}) of the inhibitor, the corrosion rate of mild steel and the degree of surface coverage were calculated using equations 1, 2 and 3 respectively [8] ;

$$IE_{exp} = (1 - W_1/W_2) \times 100 \qquad\qquad 1$$

$$CR = (W_2 - W_1)/At \qquad\qquad 2$$

$$\theta = 1 - W_1/W_2 \qquad\qquad 3$$

where W_1 and W_2 are the weight losses (g) for mild steel in the presence and absence of the inhibitor respectively, CR is the corrosion rate of mild steel in $gcm^{-2}h^{-1}$, A is the area of the mild steel (in cm^2) and t is the total period of immersion (in hours) and θ is the degree of surface coverage of the inhibitor.

2.3. Gasometric method

Gasometric methods were carried out at 303 K as described in the literature [9]. In each case, the metal coupon was inserted into the round bottom flask (containing the test solution) of the gasometer. The volumes of hydrogen gas evolved were measured after every minute until a steady value was obtained. From the volume of hydrogen gas evolved per minute, inhibition efficiencies were calculated using equation 4.

$$IE_{exp} = \left(1 - \frac{V_{Ht}^1}{V_{Ht}^o}\right) x\,100 \qquad\qquad 4$$

where V_{Ht}^1 and V_{Ht}^o are the volumes of H_2 gas evolved at time, 't' for inhibited and uninhibited solutions respectively.

2.4. Computational techniques

Single point energy calculations were carried out using AM1, PM6, PM3, MNDO and RM1 Hamiltonian in the MOPAC 2008 software for Windows [10]. The quantum chemical indices calculated were, the energy of the highest occupied molecular orbital (E_{HOMO}), the energy of the lowest unoccupied molecular orbital (E_{LUMO}), the dipole moment (μ), the total energy (TE) and the ionization potential (IP). The Mulliken and Lowdin charges (q) for nucleophilic and electrophilic attacks were computed using GAMESS computational software [11]. Correlation type and method used for the calculation was DFT while the basis set was set at 6-13G.

Statistical analyses were performed using SPSS program version 15.0 for Windows. Non-linear regression analyses were performed by unconstrained sum of squared residuals for loss function and estimation methods of Levenberg-Marquardt using SPSS program version 15.0 for Windows.

3. RESULTS AND DISCUSSION

3.1. Experimental results

Table 1 shows values of the corrosion rate of mild steel and inhibition efficiencies of various concentrations of MBDAC, HMBA and MBA.

Table 1. Inhibition efficiencies and corrosion rates of the studied anisoles on mild steel

System	CR ($gh^{-1}cm^{-2}$)		IE_{exp} (%)		IE_{exp} (Gasometric)
	303 K	333 K	303 K	333 K	**303 K**
0.5 M HCl (Blank)	0.1390	1.1250	-	-	**-**
1 x 10^{-3} M MBDAC	0.0179	0.2804	50.21	72.02	**58.33**
2 x 10^{-3} M MBDAC	0.0163	0.2463	54.23	74.11	**63.78**
3 x 10^{-3} M MBDAC	0.0155	0.2226	58.22	78.03	**68.56**
4 x 10^{-3} M MBDAC	0.0140	0.1774	62.00	80.00	**74.69**
5 x 10^{-3} M MBDAC	0.0124	0.1236	66.21	82.21	**83.04**
1 x 10^{-3} M HMBA	0.0215	0.6139	54.23	75.08	**64.36**
2 x 10^{-3} M HMBA	0.0211	0.4781	58.31	78.11	**68.34**
3 x 10^{-3} M HMBA	0.0209	0.4206	60.22	80.21	**72.34**
4 x 10^{-3} M HMBA	0.0184	0.4061	64.02	84.23	**78.07**
5 x 10^{-3} M HMBA	0.0176	0.3229	68.21	89.01	**80.88**
1 x 10^{-3} M MBA	0.0194	0.3148	44.90	45.43	**53.24**
2 x 10^{-3} M MBA	0.0179	0.2913	45.80	57.50	**63.22**
3 x 10^{-3} M MBA	0.0163	0.2472	46.50	62.61	**66.31**
4 x 10^{-3} M MBA	0.0148	0.2250	52.91	63.90	**72.30**
5 x 10^{-3} M MBA	0.0132	0.2001	54.92	71.30	**78.21**

From the results obtained, it is evident that the corrosion rate of mild steel decreases with increase in the concentration of the inhibitor but decreases with increasing temperature. These indicate that MBDAC, HMBA and MBA retarded the corrosion of mild steel in HCl solution. Table 1 also reveals that the inhibition efficiencies of MBDAC, HMBA and MBA increase with increasing concentration and with increase in temperature. These also indicate that the adsorption of the studied anisoles on mild steel surface supports the mechanism of chemical adsorption [12]. Values of inhibition efficiencies of MBDAC, HMBA and MBA calculated from gasometric measurements are also presented in Table 1. From Table 1, it can be seen that gasometric result is characterized with higher values of inhibition efficiencies compared to weight loss measurements indicating that the instantaneous inhibition efficiencies of these compounds are better than their average inhibition efficiencies.

The Arrhenius equation was used to estimate the activation energies for the corrosion of mild steel in HCl solutions containing various concentrations of MBDAC, HMBA and MBA. The Arrhenius equation can be written as follows [13];

$$CR = Aexp(-E_a/RT) \qquad\qquad 5$$

where CR is the corrosion rate of mild steel, A is the Arrhenius constant, E_a is the activation energy, R is the molar gas constant and T is the temperature. If the corrosion rates at the temperatures, T_1 (303K) and T_2 (333K) are CR_1 and CR_2 respectively, equation 5 can be simplified to the following equation.

$$\log \frac{CR_2}{CR_1} = \frac{E_a}{2.303R}\left(\frac{1}{T_1} - \frac{1}{T_2}\right) \qquad\qquad 6$$

Values of the activation energy calculated from equation 6 are recorded in Table 2.

Table 2. Values of activation energy and heat of adsorption for the studied anisoles

System	Ea (kJmol^{-1})	Q$_{ads}$ (kJ/mol)
0.5 M HCl (Blank)	38.55	-
1 x 10^{-3} M MBDAC	77.11	**19.58**
2 x 10^{-3} M MBDAC	76.09	**19.65**
3 x 10^{-3} M MBDAC	74.58	**20.66**
4 x 10^{-3} M MBDAC	71.04	**23.06**
5 x 10^{-3} M MBDAC	74.39	**27.86**
1 x 10^{-3} M HMBA	93.86	**9.45**
2 x 10^{-3} M HMBA	87.32	**9.87**
3 x 10^{-3} M HMBA	84.10	**13.75**
4 x 10^{-3} M HMBA	86.69	**9.53**
5 x 10^{-3} M HMBA	81.49	**14.95**
1 x 10^{-3} M MBA	77.99	**19.66**
2 x 10^{-3} M MBA	78.18	**18.50**
3 x 10^{-3} M MBA	76.13	**19.62**
4 x 10^{-3} M MBA	76.16	**18.81**
5 x 10^{-3} M MBA	76.17	**18.00**

The activation energies for the inhibited systems are higher than the value of 38.55 kJ/mol obtained for the blank, indicating that the corrosion of mild steel is retarded by MBDAC, HMBA and MBA. Also the activation energies are within the range of values expected for the mechanism of chemical adsorption [14]. Therefore MBDAC, HMBA and MBA are adsorbed on mild steel surface via chemical adsorption.

The heat of adsorption of MBDAC, HMBA and MBA on the surface of mild steel was calculated using the following equation [15];

$$Q_{ads} = 2.303R\left[\log\left(\frac{\theta_2}{1-\theta_2}\right) - \log\left(\frac{\theta_1}{1-\theta_1}\right)\right] x\left(\frac{T_{1X}T_2}{T_2 - T_1}\right)kJmol^{-1} \qquad\qquad 7$$

where Q$_{ads}$ is the heat of adsorption, R is the molar gas constant, θ_1 and θ_2 are the degrees of surface coverage of the inhibitor at the temperatures, T_1 and T_2 respectively. Calculated values of Q$_{ads}$ are also presented in Table 2. From the results obtained, the heats of adsorption of the studied anisoles are positive. Therefore, the adsorption of MBDAC, HMBA and MBA on mild steel surface is endothermic.

The adsorption characteristics of MBDAC, HMBA and MBA were studied by fitting data obtained for the degree of surface coverage into different adsorption isotherms. The test revealed that the best isotherms that described the adsorption behaviour of MBDAC, HMBA and MBA on mild steel surface are Frumkin and Temkin adsorption isotherms.

The Frumkin adsorption isotherm can be written as follows [16];

$$\theta/1-\theta = B.C.\exp(2a\theta) \qquad\qquad\qquad 8$$

From the logarithm of equation 8, equation 9 is obtained:

$$\log [(\theta/(1-\theta)]*[C] = \log K + 2a\theta \qquad\qquad\qquad 9$$

where θ is the degree of surface coverage, C is the concentration of the adsorbate, K is the adsorption coefficient which represents the adsorption-desorption equilibrium constant and a is an interaction parameter.

Table 3. Frumkin and Temkin parameters for the adsorption of anisoles on mild steel surface

	T (K)	Inhibitor	slope	a	logK	ΔG^0_{ads} (kJ/mol)	R^2
Frumkin	303	MBDAC	6.7931	3.40	6.5316	-47.99	0.9594
	333	MBDAC	7.8379	3.92	8.3035	-58.27	0.9636
	303	HMBA	6.9113	3.46	5.9884	-44.84	0.8319
	333	HMBA	4.6571	2.33	5.2016	-40.27	0.9895
	303	MBA	6.0704	3.04	5.9703	-44.73	0.9743
	333	MBA	8.9104	4.46	8.9326	-61.92	0.9754
Temkin	303	MBDAC	0.1864	5.36	5.8568	-48.44	0.9225
	333	MBDAC	0.1843	5.43	6.9962	-50.68	0.8762
	303	HMBA	0.1419	7.05	6.0374	-49.59	0.7335
	333	HMBA	0.13423	7.45	8.0921	-57.04	0.9701
	303	MBA	0.2217	4.51	5.2080	-44.30	0.9466
	333	MBA	0.1477	6.77	7.8152	-55.44	0.9495

Fig. 2 shows the plots of $\log [(\theta/(1-\theta)]*[C]$ versus θ and from the plots, it can be seen that values of R^2 are very close to unity. Therefore, Frumkin adsorption isotherm is applicable to the adsorption of MBDAC, HMBA and MBA on mild steel surface. Adsorption parameters deduced from the plots are recorded in Table 3. From the results obtained, it is evident that values of a are positive, which indicate the attractive behaviour of the inhibitors.

Assumptions of Temkin relate the concentration of the inhibitor to the degree of surface coverage according to equation 10 [17];

$$\exp(-2a\theta) = KC \qquad\qquad 10$$

where a is molecular interaction parameter; θ is degree of surface coverage, C is inhibitor concentration and K is equilibrium constant of the adsorption process.
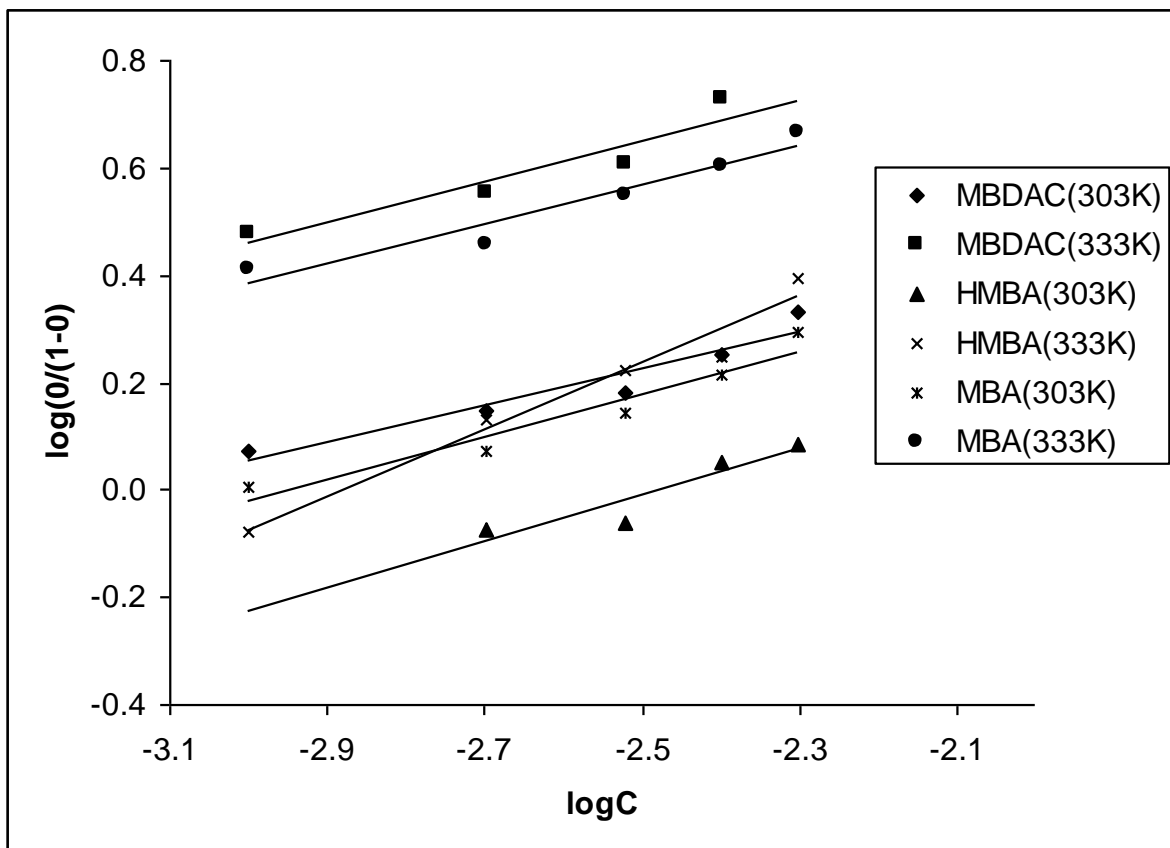

Figure 2. Frumkin isotherm for the adsorption of MBDAC, HMBA and MBA on mild steel surface

From the logarithm of both sides of equation 10, equation 11 is obtained,

$$\theta = -\frac{\ln K}{2a} - \frac{\ln C}{2a} \qquad\qquad 11$$

Fig. 3 shows Temkin isotherms for the adsorption of MBDAC, HMBA and MBA on the surface of mild steel. Adsorption parameters deduced from Temkin plots are also presented in Table 3. From the results obtained, it can be seen that values of a are also positive and compares favourably with those deduced from Frumkin adsorption isotherms.

The equilibrium constant of adsorption deduced from Frumkin and Temkin plots were used to calculate the standard free energy of adsorption of the inhibitors using equation 12 [18-19];

$$\Delta G^0_{ads} = -2.303RT\log(55.5K_{ads}) \qquad\qquad 12$$

Calculated values of ΔG^0_{ads} are presented in Table 3. The results obtained indicate that the free energies are negatively greater than the threshold value of -40 kJ/mol required for the mechanism of chemical adsorption. Therefore, the adsorption of MBDAC, HMBA and MBA on mild steel surface is spontaneous and supports the mechanism of chemical adsorption. Generally, values of ΔG^0_{ads} until -20 kJ/mol are consistent with the electrostatic interaction between the charged molecules and the charged metal (physical adsorption). Those more negative than -40 kJ/mol involve electron transfer from the inhibitor's molecule to empty d orbital of Fe in mild steel, leading to the formation of a co-ordinate type of bond (chemisorption).
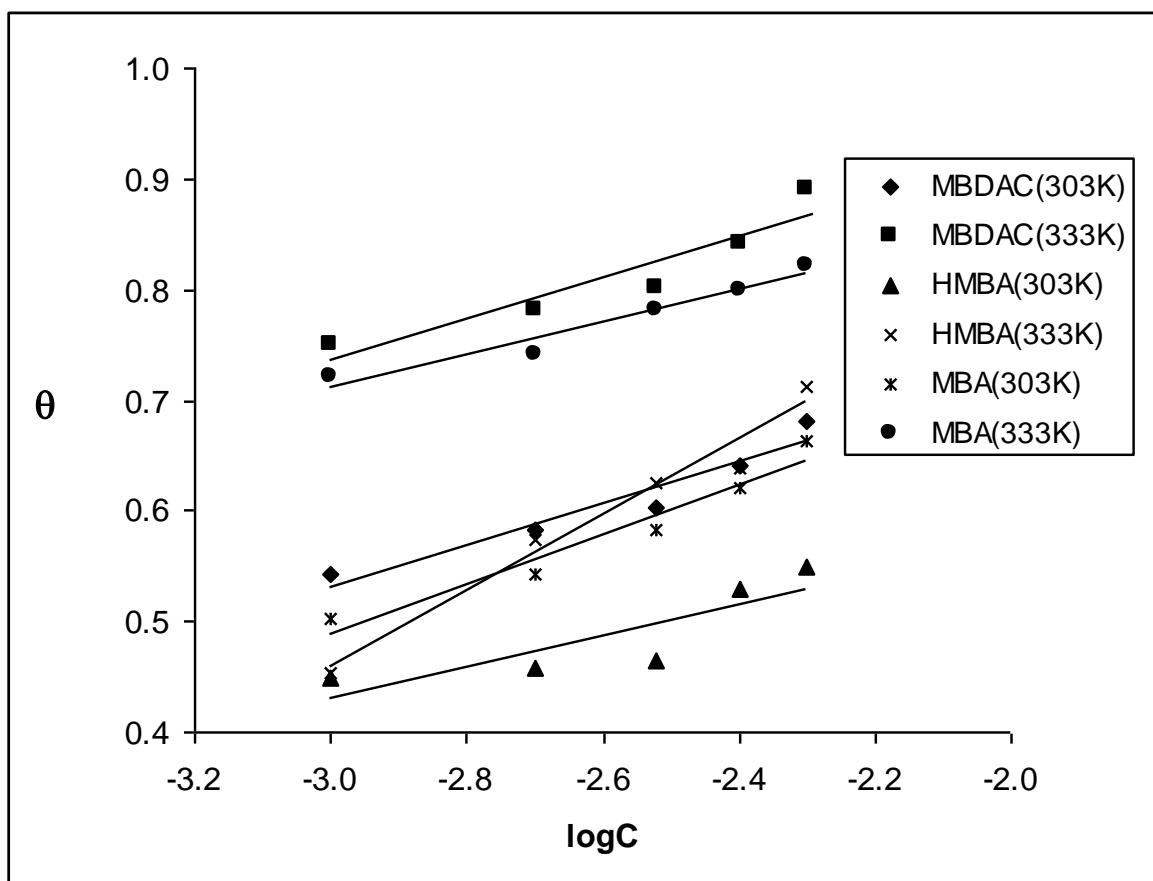

Figure 3. Temkin isotherm for the adsorption of MBDAC, HMBA and MBA on mild steel surface.

3.2. Computational study

Table 4 presents calculated quantum chemical parameters for MBDAC, HMBA and MBA in gas and aqueous phases and for various Hamiltonians (namely, PM6, PM3, AM1, RM1 and MNDO). The quantum chemical parameters included, the energy of the highest occupied molecular orbital (E_{HOMO}), the energy of the lowest unoccupied molecular orbital (E_{LUMO}), the energy gap (ΔE), the dipole moment (μ) and logP.

Table 4. Quantum chemical parameters for the studied anisoles

	Models	Gas phase					Aqueous phase				
		E_{HOMO} (eV)	E_{LUMO} (eV)	ΔE (eV)	μ (Debye)	logP	E_{HOMO} (eV)	E_{LUMO} (eV)	ΔE (eV)	μ (Debye)	E_{diel} (eV)
MBDAC	PM6	-9.39	-0.46	8.93	2.83	2.85	-9.38	-0.49	8.89	3.67	-0.84
	PM3	-9.48	-0.49	8.99	2.14	2.85	-9.31	-0.43	8.88	2.68	-0.55
	AMI	-9.45	-0.33	9.12	2.33	2.85	-9.33	-0.31	9.02	2.65	-0.61
	RMI	-9.36	-0.16	9.20	2.45	2.85	-9.22	-0.11	9.11	2.80	-0.60
	MNDO	-9.57	-0.53	9.04	2.19	2.85	-9.37	-0.38	8.99	2.82	-0.51
HMBA	PM6	-9.14	-0.38	8.06	2.56	2.69	-9.19	-1.22	7.97	3.37	-0.42
	PM3	-9.29	-0.65	8.63	1.97	2.69	-9.19	-0.73	8.46	2.69	-0.24
	AMI	-9.21	-0.59	8.62	1.85	2.69	-9.16	-0.67	8.49	2.78	-0.28
	RMI	-9.11	-0.47	8.64	1.75	2.69	-9.04	-0.53	8.51	3.02	-2.28
	MNDO	-9.31	-0.72	8.59	1.45	2.69	-9.17	-0.67	8.5	3.02	-0.24
MBA	PM6	-9.71	-0.59	9.12	3.76	2.86	-9.87	-0.82	9.05	4.79	-0.56
	PM3	-9.73	-0.44	9.29	2.67	2.86	-9.79	-0.56	9.23	3.36	-0.32
	AMI	-9.68	-0.34	9.33	2.72	2.86	-9.76	-0.48	9.28	3.33	-0.36
	RMI	-9.55	-0.16	9.39	2.75	2.86	-9.62	-0.27	9.35	3.41	-0.35
	MNDO	-9.71	-0.49	9.23	2.53	2.86	-9.70	-0.51	9.19	3.12	-0.30

According to the frontier molecular orbital theory, chemical reactivity can be considered in terms of interaction between the E_{HOMO} and the E_{LUMO}. E_{HOMO} indicates the tendency of a molecule to donate electron while E_{LUMO} indicates the tendency of a molecule to accept a lone pair of electron [20]. Therefore, higher value of E_{HOMO} and lower value of E_{LUMO} signify better inhibition efficiency. A close examination of the experimental results reveals that based on increasing values of E_{HOMO} and on decreasing value of E_{LUMO}, the inhibition efficiency of the studied anisoles is expected to follow the order, HMBA > MBDAC > MBA. This trend is consistent with results obtained from experiments. Also from the structures of the three inhibitors, it can be stated that the introduction of -OH functional group to the 4-methoxybenzaldehyde molecules leads to increasing value of E_{HOMO} and a corresponding decrease in the values of the E_{LUMO} and ΔE (E_{L-H}). Consequently, a corresponding increase in the adsorption of HMBA over MBA and MBDAC (hence inhibition efficiency) is expected. Also, replacement of the =O group in 4-methoxybenzaldehyde by methylenecarbamic acid (NCH_2CO_2H) enhances the adsorption of MBDAC over MBA by increasing the value of E_{HOMO} and a corresponding decrease in the value of E_{LUMO}

The ΔE of a molecule is defined as the difference between the E_{LUMO} and the E_{HOMO} (i.e $\Delta E = E_{LUMO} - E_{HOMO}$). The ΔE of a molecule is a measure of the hardness or softness of a molecule [21]. Hard molecules are characterized by larger values of ΔE and vice versa. However, hard molecules are less reactive than soft molecules because the larger the gap between the last occupied orbital and the first virtual orbital, the more it is difficult for intermolecular electron transfer to proceeds. From the calculated values of the ΔE, the trend for the variation of the inhibition efficiency of the studied anisoles with decreasing value of ΔE, is similar to that deduced from experimental data.

μ is the measure of the polarity in a bond and is related to the distribution of electron in a molecule [22]. Although, there are some inconsistencies on the use of μ as a predictor for the direction of a corrosion inhibition reaction, it is generally agreed that the adsorption of polar compounds possessing high dipole moments on the metal surface should lead to better inhibition. Comparison of the results obtained from quantum chemical calculations (for both gas and aqueous phases) with experimental inhibition efficiencies indicated that the inhibition efficiencies of the inhibitors increase with decreasing value of μ.

LogP accounts for the hydrophobicity of a molecule. This implies that the higher the value of logP, the more hydrophobic is the molecule hence water solubility is expected to decrease with increasing value of logP. From the point of view of corrosion inhibition process, the processes of inhibition that are affected by hydrophobicity are not well established. However, it is most probably that hydrophobicity can be used to predict the mechanism of formation of the oxide/hydroxide layer on the metal surface (which reduces the corrosion process drastically) [23]. From the results obtained, the inhibition efficiency of the studied inhibitors is found to increase with increasing value of logP. This trend supports experimental results.

Table 5. Values of R^2 for the variation of IE_{exp} with some gas phase (aqueous phase) quantum chemical parameters

	E_{HOMO} (eV)	E_{LUMO} (eV)	ΔE (eV)	μ (Debye)	logP
PM6	0.9974(0.9431)	0.9864(0.9944)	0.8664(0.8444)	0.9194(0.9114)	**0.7779**
PM3	0.9965(0.9046)	0.9051(0.9907)	0.9948(0.9948)	0.9293(0.7558)	**0.7779**
AM1	0.9990(0.9499)	0.7024(0.9973)	0.9383(0.9548)	0.9937(0.7996)	**0.7779**
RM1	0.9904(0.9620)	0.7329(0.9758)	0.9144(0.9329)	0.9405(0.8210)	**0.7779**
MNDO	0.9640(0.9854)	0.8627(0.9937)	0.9388(0.9351)	0.9479(0.8234)	**0.7779**

Fig. 4 shows plots for the variation of IE_{exp} with E_{HOMO}, E_{LUMO}, ΔE, μ and logP for MBDAC, HMBA and MBA. The plots were developed from gas phase AM1 data. Plots for aqueous phase and for other Hamiltonians are not presented but calculated values of R^2 for both gas and aqueous phases are recorded in Table 5. From the plots and from the presented values of R^2, it is evident that correlations between IE_{exp} and the calculated quantum chemical parameters (i.e E_{HOMO}, E_{LUMO}, ΔE, μ and logP) are excellent. This implies that the E_{HOMO}, E_{LUMO}, ΔE, μ and logP are good quantum chemical predictors for the inhibition of the corrosion of mild steel by MBDAC, HMBA and MBA.

The ionization energy (IP) and the electron affinity (EA) of the inhibitors were calculated using the finite difference approximation, which can be expressed as follow [24];

$$IP = E_{(N-1)} - E_{(N)} \qquad\qquad 13$$

$$EA = E_{(N)} - E_{(N+1)} \qquad\qquad 14$$

where $E_{(N+1)}$, $E_{(N)}$ and $E_{(N-1)}$ are the ground state energies of the molecule with N+1, N and N-1 electrons respectively. Also, using the finite difference approximation, the global hardness, η and softness, S were evaluated from the following equations [25];

$$\eta = [(E_{(N-1)} - E_{(N)}) - (E_{(N)} - E_{(N+!)})] \qquad\qquad 15$$
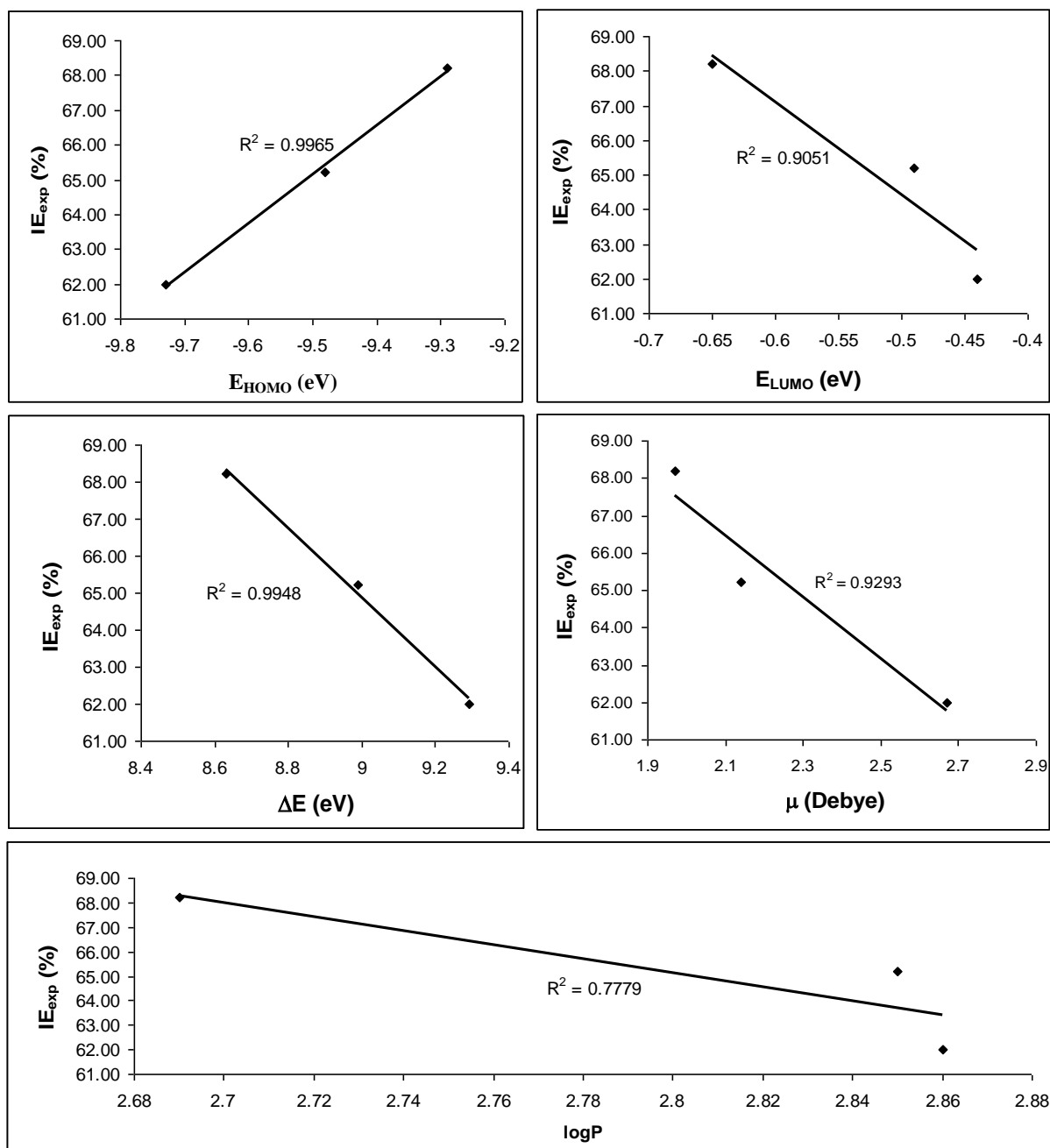
$$S = 1/[(E_{(N-1)} - E_{(N)}) - (E_{(N)} - E_{(N+!)})] \qquad\qquad 16$$

Figure 4. Variation of experimental inhibition efficiency of the studied anisoles with E_{HOMO}, E_{LUMO}, ΔE, μ and logP for gas phase AM1 Hamiltonian

The electronegativity, χ of the inhibitors was also calculated using the following expression [26];

$$\chi = (IP + EA)/2 \qquad\qquad 17$$

In order to calculate the fraction of electron transferred (δ), equation 18 was used [27];

$$\delta = (\chi_{Fe} - \chi_{inh})/2(\eta_{Fe} + \eta_{inh}) \qquad\qquad 18$$

where χ_{Fe} and χ_{inh} are the electronegativity of Fe and that of the inhibitor respectively while η_{Fe} and η_{inh} are the global hardness of Fe and the inhibitor respectively. In this study, the theoretical values of $\chi_{Fe} = 7ev$ and $\eta_{Fe} = 0$ were used for the computation of δ values for the various Hamiltonians.

Table 6. Quantum chemical descriptors for the studied inhibitors

| | Models | Gas phase | | | | | | Aqueous phase | | | | | |
		IE (eV)	EA (eV)	χ (eV)	S (/eV)	η (eV)	δ	IP (eV)	EA (eV)	χ (eV)	S (/eV)	η (eV)	δ
MBDAC	PM6	9.01	1.14	5.08	0.13	7.87	0.12	6.75	3.21	5.08	0.13	7.87	0.12
	PM3	9.17	1.04	5.11	0.12	8.13	0.12	6.84	3.04	5.11	0.12	8.13	0.12
	AMI	9.22	0.69	4.27	0.10	9.91	0.14	6.76	3.00	4.96	0.12	9.90	0.14
	RMI	8.85	0.84	4.85	0.13	8.01	0.14	6.61	2.84	4.85	0.12	8.00	0.13
	MNDO	9.49	1.18	5.34	0.12	8.31	0.10	6.74	3.09	5.34	0.12	8.33	0.10
HMBA	PM6	8.59	1.63	5.11	0.14	6.96	0.14	6.49	4.00	5.11	0.14	6.94	0.14
	PM3	8.83	1.07	4.95	0.13	7.76	0.13	6.59	3.39	4.95	0.13	7.75	0.13
	AMI	8.67	1.12	4.90	0.13	7.55	0.14	6.50	3.40	4.90	0.13	7.58	0.14
	RMI	8.56	1.00	4.78	0.13	7.56	0.15	6.36	3.27	4.78	0.13	7.58	0.15
	MNDO	8.75	1.28	5.02	0.13	7.47	0.13	6.48	3.44	5.02	0.13	7.46	0.13
MBA	PM6	9.13	1.16	5.15	0.13	7.97	0.12	7.10	3.64	5.15	0.13	8.00	0.12
	PM3	9.29	0.86	5.08	0.12	8.43	0.11	7.18	2.91	5.08	0.12	8.40	0.11
	AMI	9.14	0.87	5.01	0.12	8.27	0.12	7.07	3.20	5.01	0.12	8.26	0.12
	RMI	9.00	0.70	4.85	0.12	8.30	0.13	6.93	3.00	4.85	0.12	8.33	0.13
	MNDO	9.15	1.04	5.10	0.12	8.11	0.12	6.98	3.26	5.10	0.12	8.13	0.12

Calculated values of IE, EA, η, S and δ for the studied inhibitors are presented in Table 6. From the results obtained, it can be seen that the IE_{exp} increases with increasing IE, S, and δ and the order of the increase is consistent with experimental data. On the other hand, the IE and η of the inhibitors were found to decrease with increase in the value of IE_{exp}. These indicate that the best inhibitor is characterized by highest values of IE, S, and δ and lowest values of IE and η.

It has been found that not only can the inhibitor's molecule donate electron to the metal ion but it is possible for the inhibitor to accept electron from the d orbital of iron leading to the formation of a

feedback bond. In order to establish the formation of a feedback bond, multiple regressions were performed between the experimental inhibition efficiency and the energies of the frontier molecular orbitals. The regression yielded equations 19 to 23 for PM6, PM3, AM1, RM1 and MNDO for gas phase calculations.

$$IE_{exp} = 19.30E_{HOMO} - 22.83E_{LUMO} + 234.98 \qquad\qquad 19$$

$$IE_{exp} = 11.92E_{HOMO} - 4.59E_{LUMO} + 175.97 \qquad\qquad 20$$

$$IE_{exp} = 13.90E_{LUMO} - 1.29E_{LUMO} + 196.99 \qquad\qquad 21$$

$$IE_{exp} = 16.89E_{HOMO} - 3.95E_{LUMO} + 223.98 \qquad\qquad 22$$

$$IE_{exp} = 30.24E_{HOMO} - 25.59E_{LUMO} + 368.18 \qquad\qquad 23$$

From the above equations, it can be seen that the coefficients of E_{HOMO} are positive while those of E_{LUMO} are negative. These indicate that the formation of a feedback bond is favoured by increasing value of E_{HOMO} and decreasing value of E_{LUMO}. Similar deductions are apparent from aqueous phase data (equations not shown). However, when other quantum chemical parameters were used in carrying out multiple regressions, it was impossible to obtain equations such as those listed above. This suggests that the corrosion inhibition potentials of the studied inhibitors are complex functions of more quantum chemical/mechanical variables. Therefore, a non linear model (equation 24), which was first proposed by Lukovits *et al*, [28] for the study of interaction of corrosion inhibitors with metal surface in acidic solutions was used. This non linear model can be written as follows,

$$IE_{Theor}(\%) = \frac{(Ax_j + B)C_i}{1 + (Ax_j + B)C_i} \times 100 \qquad\qquad 24$$

where IE_{Theor} is the theoretical inhibition efficiency, A is a regression coefficient, B is a regression constant, C_i is the experimental concentration of the inhibitor and x_i is a quantum chemical index of the molecule, i. Application of equation 24 yielded equations 25 to 29 for gas phase data and equations 30 to 34 for aqueous phase data.

$$IE_{Theor} = \frac{(E_{HOMO} + 0.9544E_{LUMO} + 0.9635\Delta E + \mu + 103.7541*logP)*C_i \times 100}{(1+(E_{HOMO} + 0.9544E_{LUMO} + 0.9635\Delta E + \mu + 103.7541*logP)*C_i} \qquad 25$$

$$IE_{Theor} = \frac{(E_{HOMO} + 0.9671E_{LUMO} + 0.8966\Delta E + \mu + logP + 186.86)*C_i \times 100}{(1+(E_{HOMO} + 0.9671E_{LUMO} + 0.8966\Delta E + \mu + logP + 186.86)*C_i} \qquad 26$$

$$IE_{Theor} = \frac{(E_{HOMO} + 0.88E_{LUMO} + \Delta E + 1.065\mu + logP + 89.68)*C_i \times 100}{(1+(E_{HOMO} + 0.88E_{LUMO} + \Delta E + 1.065\mu + logP + 89.68)*C_i} \qquad 27$$

$$IE_{Theor} = \frac{(E_{HOMO} + 0.8451E_{LUMO} + \Delta E + 1.264\mu + logP + 102.25)*C_i \times 100}{(1+(E_{HOMO} + 0.8451E_{LUMO} + \Delta E + 1.264\mu + logP + 102.25)*C_i} \qquad 28$$

$$IE_{Theor} = \frac{(1.599E_{HOMO} + 0.8502E_{LUMO} + \Delta E +\mu+logP + 124.42)*C_i \times 100}{(1+(1.599E_{HOMO} + 0.8502E_{LUMO} + \Delta E +\mu+logP + 124.42)*C_i} \qquad 29$$

$$IE_{exp} = \frac{(E_{HOMO} + 0.9608E_{LUMO} +0.9648\Delta E + \mu +logP+103.86) \times C_i \times 100}{(1+(E_{HOMO} + 0.9608E_{LUMO} +0.9648\Delta E + \mu +logP+103.86)*C_i)} \qquad 30$$

$$IE_{exp} = \frac{(E_{HOMO} + 0.981E_{LUMO} +0.898\Delta E + \mu +logP+178.25) \times C_i \times 100}{(1+(E_{HOMO} + 0.981E_{LUMO} +0.898\Delta E + \mu +logP+178.25)*C_i)} \qquad 31$$

$$IE_{exp} = \frac{(E_{HOMO} + 0.963E_{LUMO} +0.910\Delta E + \mu +logP+168.82) \times C_i \times 100}{(1+(E_{HOMO} + 0.963E_{LUMO} +0.910\Delta E + \mu +logP+168.82)*C_i)} \qquad 32$$

$$IE_{exp} = \frac{(0.965E_{HOMO} + 0.934E_{LUMO} + \Delta E + \mu +logP+77.24) \times C_i \times 100}{(1+(0.965E_{HOMO} + 0.934E_{LUMO} + \Delta E + \mu +logP+77.24)*C_i)} \qquad 33$$

$$IE_{exp} = \frac{(E_{HOMO} + 0.919E_{LUMO} +0.882 \Delta E + \mu +logP+256.98) \times C_i \times 100}{(1+(E_{HOMO} + 0.919E_{LUMO} +0.882 \Delta E + \mu +logP+256.98)*C_i)} \qquad 34$$

In Table 7, we present the theoretical inhibition efficiencies for the inhibitors in gas and aqueous phases.

Fig. 5 is a representative plot, showing the pattern of variation of IE_{theor} with IE_{exp} for MBDAC in gas phase. Plots for other inhibitors in gas and aqueous phases are not shown but calculated values of R^2 are presented in Table. 8. From the calculated values of R^2, it is evident that correlations between IE_{exp} and IE_{Theor} are also excellent. Therefore, quantum chemical parameters can be used to predict the inhibition potentials of anisoles.

The local selectivity of the inhibitors was analysed using the Fukui function which can be defined as follows [29];

$$f(r) = [(\delta \Upsilon / \delta v(r))]_N \qquad\qquad 35$$

where $v(r)$ is the external potential and the functional derivative must be taken at constant number of electrons.
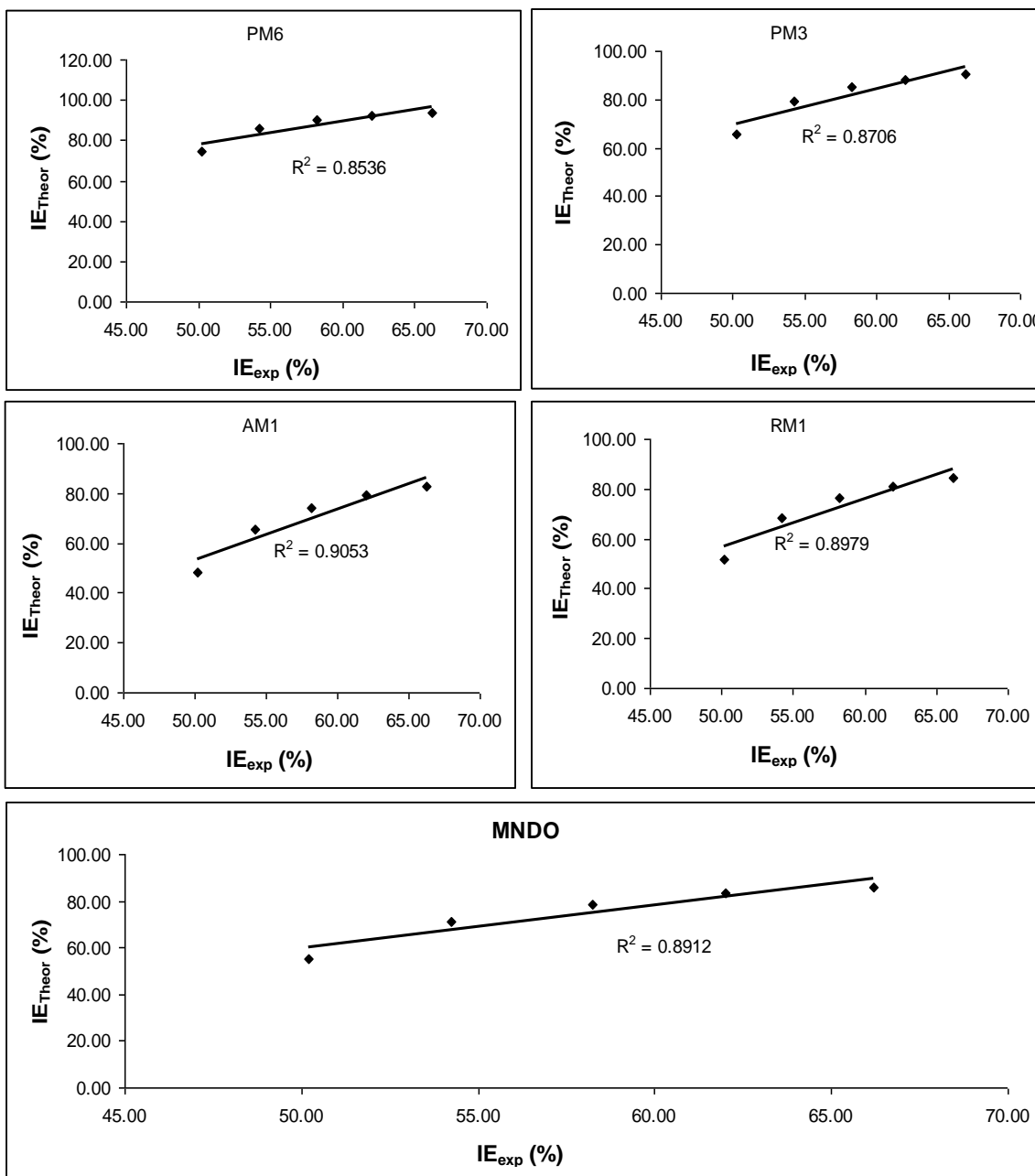

Figure 5. Variation of theoretical inhibition efficiency with experimental inhibition efficiency of MBDAC

Table 7. Theoretical inhibition efficiencies of MBDAC, HMBA and MBA for gas and aqueous phases

	C (M)	Gas phase					Aqueous phase				
		PM6	PM3	AM1	RM1	MNDO	PM6	PM3	AM1	RM1	MNDO
MBDAC	1×10^{-3}	74.83	65.51	48.56	51.9	55.21	51.24	64.09	62.86	44.26	72.02
	2×10^{-3}	85.60	79.16	65.37	68.34	71.14	67.76	78.12	77.20	61.36	83.73
	3×10^{-3}	89.92	85.07	73.90	76.40	78.71	75.92	84.26	83.55	70.43	88.55
	4×10^{-3}	92.24	88.37	79.06	81.19	83.14	80.78	87.71	87.13	76.05	91.16
	5×10^{-3}	93.7	90.47	82.52	84.36	86.04	84.19	89.92	89.43	79.88	92.79
HMBA	1×10^{-3}	73.68	65.44	48.25	51.52	55.00	51.01	64.08	62.86	43.59	72.03
	2×10^{-3}	84.84	79.11	65.09	68.01	70.97	67.56	78.11	77.19	60.71	83.74
	3×10^{-3}	89.36	85.03	73.66	76.13	78.57	75.75	84.26	83.55	69.86	88.54
	4×10^{-3}	91.80	88.34	78.85	80.96	83.02	80.64	87.71	87.13	75.56	91.15
	5×10^{-3}	93.73	90.50	82.58	84.41	86.13	83.89	89.92	89.43	79.44	92.79
MBA	1×10^{-3}	74.94	65.58	48.66	51.99	55.40	51.57	64.20	62.99	44.53	72.06
	2×10^{-3}	85.67	79.22	65.47	68.41	71.30	68.05	78.20	77.29	61.62	83.76
	3×10^{-3}	89.97	85.11	73.98	76.46	78.84	76.16	84.33	83.62	70.66	88.55
	4×10^{-3}	92.28	88.40	79.13	81.24	83.25	80.99	87.77	87.19	76.25	91.16
	5×10^{-3}	93.73	90.50	82.58	84.41	86.13	84.19	89.97	89.48	80.06	92.80

Table 8. R^2 values for IE_{exp} and IE_{Theor} of MBDAC, HMBA and MBA in gas phase (aqueous phase).

	MBDAC	**HMBA**	**MBA**
PM6	0.8586(0.9020)	0.8666(0.9020)	0.8534(0.8987)
PM3	0.8706(0.8733)	0.8720(0.8734)	0.8704(0.8731)
AM1	0.9053(0.8756)	0.9092(0.8758)	0.9050(0.8755)
RM1	0.8979(0.9146)	0.9023(0.9161)	0.8979(0.9140)
MNDO	0.8912(0.8583)	0.8946(0.8584)	0.8907(0.8585)

However, in this study, the Fukui functions for electrophilic and nucleophilic attacks were calculated using the finite difference approximation, which can be expressed as follows [30];

$$f^+ = (\delta\rho(r)/\delta N)^+_{\upsilon} = q_{(N+1)} - q_{(N)} \qquad\qquad 36$$

$$f^- = (\delta\rho(r)/\delta N)^-_{\upsilon} = q_{(N)} - q_{(N-1)} \qquad\qquad 37$$

where ρ, $q_{(N+1)}$, $q_{(N)}$ and $q_{(N-1)}$ are the density of electron and the Mulliken/Lowdin charge of the atom with N+1, N and N-1 electrons respectively.

Table 9. Fukui and global softness indices for nucleophillic and electrophillic attacks in MBDAC, HMBA and MBA calculated from Mulliken (Lowdin) charges

|	Atom No	f⁺ (|e|)	f⁻ (|e|)	S⁺ (eV|e|)	S⁻ (eV|e|)
MBDAC	1 C	-0.0564(-0.0733)	-0.0339(-0.0379)	-0.0068(-0.0088)	-0.0041(-0.0045)
	2 C	-0.0102(-0.0044)	-0.0184(-0.0188)	-0.0012(-0.0005)	-0.0022(-0.0023)
	3 C	-0.0876-0.1108)	-0.0468(0.0532)	-0.0105(-0.0133)	-0.0056(-0.0064)
	4 C	-0.0134(-0.0090)	-0.0142(-0.0118)	-0.0016(-0.0011)	-0.0017(-0.0014)
	5 C	-0.0539(-0.0644)	-0.0292(-0.0331)	-0.0065(-0.0077)	-0.0035(-0.0040)
	6 C	-0.0294(-0.0339)	0.0063(0.0133)	-0.0035(-0.0041)	0.0008(0.0016)
	7 C	-0.1222(-0.1515)	-0.1041(-0.1216)	-0.0147(-0.0182)	-0.0125(-0.0146)
	8 O	-0.0284(-0.0290)	-0.0283(-0.0309)	-0.0034(-0.0035)	-0.0034(-0.0037)
	9 N	-0.1244(-0.1510	-0.2478(-0.3128)	-0.0149(-0.0181)	-0.0297(-0.0375)
	10 C	-0.0034(-0.0078)	-0.0272(-0.0326)	-0.0004(-0.0009)	-0.0033(-0.0039)
	11 C	-0.0109(-0.0022)	-0.0026(0.0074)	-0.0013(-0.0003)	-0.0003(0.0009)
	12 O	-0.0427(-0.0408)	-0.0718(-0.0706)	-0.0051(-0.0049)	-0.0086(-0.0085)
	13 O	-0.0011-0.0022)	0.0074(0.0054)	-0.0001(-0.0003)	0.0009(0.0006)
	14 C	0.0007(-0.004)	0.0014(-0.0023)	0.0001(-0.0005)	0.0002(-0.0003)
HMBA	1 C	-0.0565(-0.0707)	-0.0285(-0.0317)	-0.0073(-0.0092)	-0.0037(-0.0041)
	2 C	-0.0164(-0.0134)	-0.0196(-0.0186)	-0.0021(-0.0017)	-0.0025(-0.0024)
	3 C	-0.0740(-0.1010)	-0.0627(-0.0819)	-0.0096(-0.0131)	-0.0081(-0.0106)
	4 C	-0.0316(-0.0259)	-0.0210(-0.0142)	-0.0041(-0.0034)	-0.0027(-0.0018)
	5 C	-0.0641(-0.0734)	-0.0565(-0.0583)	-0.0083(-0.0095)	-0.0073(-0.0076)
	6 C	-0.0242(-0.0232)	-0.0050(0.0031)	-0.0031(-0.0030)	-0.0006(0.0004)
	7 C	-0.1805(-0.2185)	-0.0976(-0.1191)	-0.0235(-0.0284)	-0.0127(-0.0155)
	8 O	-0.0372(-0.0352)	-0.0439(-0.0441)	-0.0048(-0.0046)	-0.0057(-0.0057)
	9 O	-0.0255(-0.0233)	-0.0263(-0.0251)	-0.0033(-0.0030)	-0.0034(-0.0033)
	10 O	-0.1513(-0.1578)	-0.3202(-0.3540)	-0.0197(-0.0205)	-0.0416(-0.0460)
	11 C	0.0022(-0.0020)	0.0022(-0.0015)	0.0003(-0.0003)	0.0003(-0.0002)
MBA	1 C	-0.0585(-0.0745)	-0.0478(-0.0545)	-0.0070(-0.0089)	-0.0057(-0.0065)
	2 C	-0.0149(-0.0101)	-0.0148(-0.0129)	-0.0018(-0.0012)	-0.0018(-0.0015)
	3 C	-0.0927(-0.1168)	-0.0683(-0.0802)	-0.0111(-0.0140)	-0.0082(-0.0096)
	4 C	-0.0092(-0.0023)	-0.0151(-0.0122)	-0.0011(-0.0003)	-0.0018(-0.0015)
	5 C	-0.0631(-0.0804)	-0.0362(-0.0427)	-0.0076(-0.0097)	-0.0043(-0.0051)
	6 C	-0.0297(-0.0323)	0.0034(0.0142)	-0.0036(-0.0039)	0.0004(0.0017)
	7 C	-0.1711(-0.2067)	-0.0969(-0.1199)	-0.0205(-0.0248)	-0.0116(-0.0144)
	8 O	-0.0302(-0.0310)	-0.0404(-0.0453)	-0.0036(-0.0037)	-0.0049(-0.0054)
	9 O	-0.1471(-0.1536)	-0.3190(-0.3527)	-0.0177(-0.0184)	-0.0383(-0.0423)
	10 C	0.0009(-0.0041)	0.0020(-0.0029)	0.0001(-0.0005)	0.0002(-0.0003)

HOMO **LUMO**
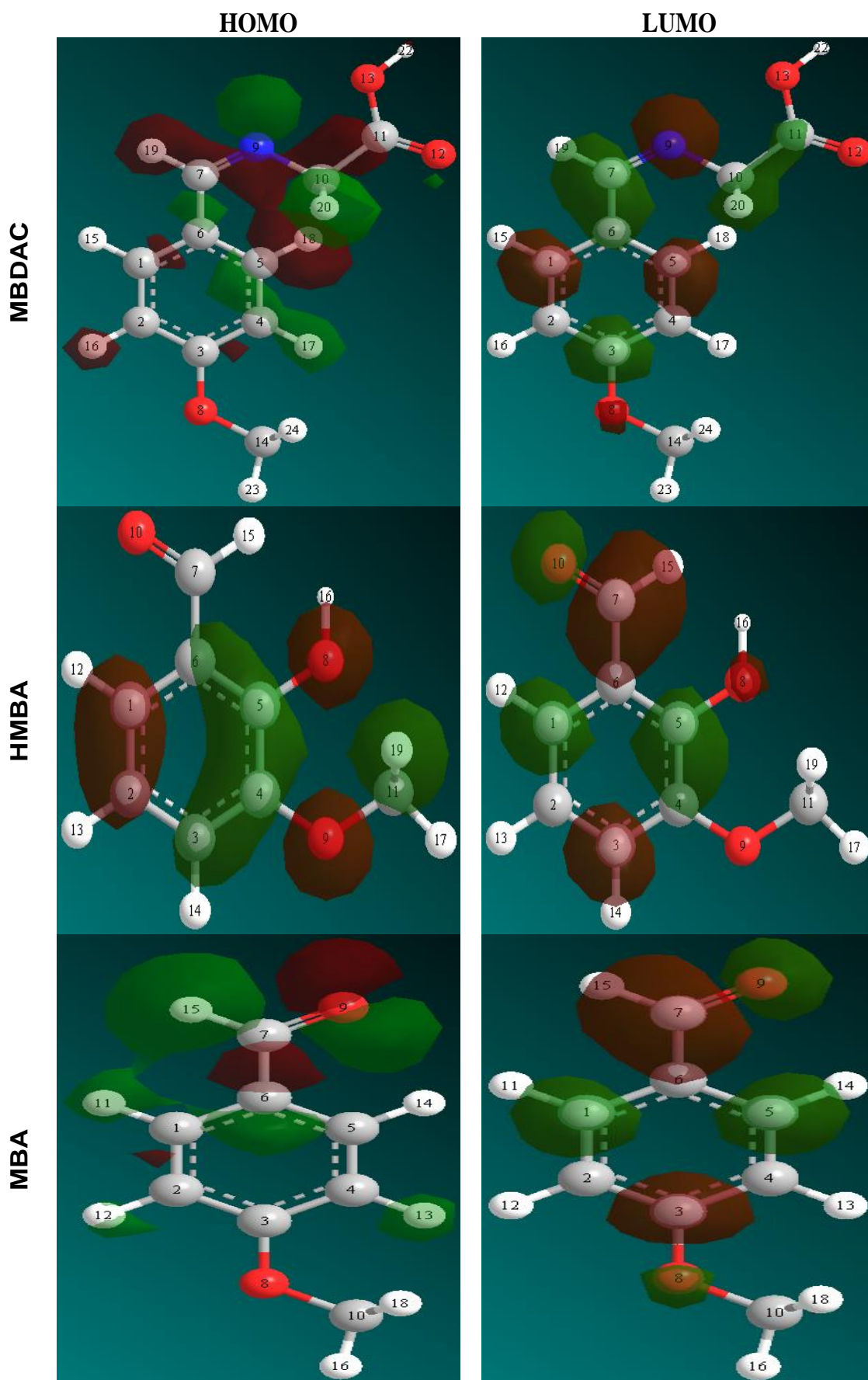
Figure 6. Frontier molecular orbital of MBDAC, HMBA and MBA

The product of the Fukui function and the global softness (S) is defined as the local softness of the inhibitors and for electrophilic and nucleophilic attacks, the local softness can be expressed as shown below [31];

$$s^+ = (f^+)S \qquad\qquad 38$$

$$s^- = (f^-)S \qquad\qquad 39$$

In analysing the Fukui function and the local softness parameters, it is significant to note that the site for electrophilic attack is the site where the values of f^+ and s^+ are maximum [32]. On the other hand, the site for nucleophilic attack is the site where f^- and s^- are maximum. Calculated values of f^+, f^- , s^+ and s^- are presented in Table 9. From the results obtained, it is evident that the sites for electrophilic and nucleophilic attacks in the studied anisoles are in their respective enol bonds (i. e C14-O8, C11-O9 and C10-O8 in MBDAC, HMBA and MBA respectively).

In Fig. 6, molecular orbitals of MBDAC, HMBA and MBA showing, the HOMO and the LUMO (green represent positive while maroon represent negative) are presented. Fig. 6 reveals that the enol bonds are the likely sites for attack, which is consistent with the findings deduced from Fukui function analyses.

4. CONCLUSIONS

From the results and findings of the studied, it can be concluded that MBDAC, HMBA and MBA are good inhibitors for the corrosion of mild steel in HCl solution. The inhibitory potentials of the inhibitors are due to the transfer of electron from the inhibitor to Fe in mild steel or vice versa. From experimental and theoretical data, the trend for the variation of the inhibition efficiencies of the compounds is HMBA > MBDAC>MBA. Therefore, the use of quantum chemical parameters is appropriate in modelling the inhibitory behaviour of the studied anisoles.

Reference

1. N.O. Eddy, U.J. Ibok, U. J. and E.E. Ebenso, *J. Appl. Electrochem.* 40 (2010) 445.
2. O.K. Abiola, N.C. Oforka, E.E. Ebenso and N.M. Nwinuka, *Anti-Corrosion Methods & Materials*, 54(4) (2007) 219.
3. M. Finsgar, A. Lesar, A. Kokaij, I.A. Milosev, *Electrochimica Acta.* 53(2008) 8287.
4. I.B. Obot, N.O. Obi-Egbedi, S.A. Umoren, E.E. Ebenso, *Int. J. Electrochem. Sci.* 5 (2010) 994.
5. I.B. Obot, N.O. Obi-Egbedi, S.A. Umoren, *Int. J. Electrochem. Sci.* 4 (2009) 863.
6. D. Gopi, K. M. Govindaraju, V. Collins, Arun Prakash, V. Manivannan and L. Kavitha *J. Appl. Electrochem.* 39(2) (2009) 269.
7. M.G. Sethuran & P.B. Raja, *Pigment & Resin Technology*, 34(6) (2005) 327.
8. A.O. Odiongenyi, S.A. Odoemelam, and N.O. Eddy, *Portugaliae Electrochimica Acta* 27(1) (2009) 33.
9. S.A. Umoren, & E.E. Ebenso, *Pigment and Resin Technology* 37(3) (2008)173.

10. Steward, J. P. MOPAC (2009). Steward computational Chemistry, Version 9.069W. HTTP://OpenMOPAC.net

11. M.W. Schmidt, K.K. Baldridge, J.A. Boatz, S.T. Elbert, M.S. Gordon,J.H. Jensen, S. Koseki, N. Matsunaga, K.A. Nguyen, S.J. Su, T.L. Windus, M. Dupus, J.A. Montgomery,*J.Comp.Chem.* (1993) 1347.

12. E.A. Noor, (2009). *J. Appl. Electrochem*. 39 (2009) 1465.

13. N.O. Eddy and P.A.P. Mamza, *Portugaliae Electrochimica. Acta*. 27(2) (2009) 20.

14. N.O. Eddy and E.E. Ebenso, *Pigment and Resin Technology* 39(2) (2010) 77.

15. N.O. Eddy, S.A. Odoemelam, A.O. Odiongenyi, *J. Appl. Electrochem*. 39(6) (2009) 849.

16. G. Moreit, G. Quartarone, A. Tassan, A. Zingales, *Electrochimica Acta* 41(13) (1996) 1971.

17. M.A. Quraishi, K. Hariom, K. Sharma, *Mater. Chem. Phys*. 78 (2002) 18.

18. K.C. Emregul, E. Duzgun, & O. Atakiol, *Corrosion Science*, 48 (2006) 3243.

19. B. Da-Quan Zhanga, Qi-Rui Caia, H. Xian-Ming, G. Li-Xin, Guo-Ding Zhou, *Mater. Chem. Phys*. 112 (2008) 353.

20. E.E. Ebenso, T. Arslan, F. Kandemirli, N. Caner, I. Love, *Int. J. Quant. Chem*. 110 (2010) 1003.

21. M. Sahin, G. Gece, F. Karci and S. Bilgic, *J. Appl. Electrochem.* 38 (2008) 809.

22. H. Tanak and M. Yavuz, *J. Molecular Modelling* 16 (2010) 235.

23. N.O. Eddy and E.E. Ebenso, *J. Molecular Modeling* 16 (2010) 1291.

24. N.O. Eddy, *Molecular Simulation*. 35(5)(2010) 354-363.

25. N.O. Eddy, F.E. Awe, C.E. Gimba, N.O. Ibisi and E.E. Ebenso, *Int. J. Electrochem. Sci*. 6(2011) 931.

26. B. Gomez, N.V.Likhanova, M.A. Dominguez, R.A. Martinez-Palou, A. Vela and J.L. Gazquez, *J. Phys. Chem. B* 110 (2006) 8928.

27. H. Wang, X. Wang, H. Wang, L. Wang and A. Liu, *J. Mol. Model*. 13(2007)147.

28. I.Lukovits, A. Shaban and E. Kalman, *Russian J. Electrochem.* 39 (2003) 177.

29. P. Fuentealba, P. Perez and R. Contreras, *J. Chem. Phys.* 113 (7) (2000) 2544.

30. E.E. Ebenso, D.A. Isabirye and N.O. Eddy, *Int. J. Mol. Sci.* 11 (2010) 2473.

31. N.O. Eddy, and B.I. Ita, *Int. J. Quantum Chemistry* (2010) DOI: 10.1002/qua

32. N.O. Eddy , B.I. Ita, N.E. Ibisi and E.E. Ebenso, *Int. J. Electrochem. Sci*. 6(2011) 1027.